SUPPLEMENTARY DATA

Molecular basis for protein histidine N1-specific methylation of the "His-x-His" motifs by METTL9

Wentao Zhao, Yang Zhou, Caiyi Li, Yucong Bi, Keyun Wang, Mingliang Ye and Haitao Li*

-SUPPLEMENTARY FIGURES AND LEGENDS

-SUPPLEMENTARY TABLES

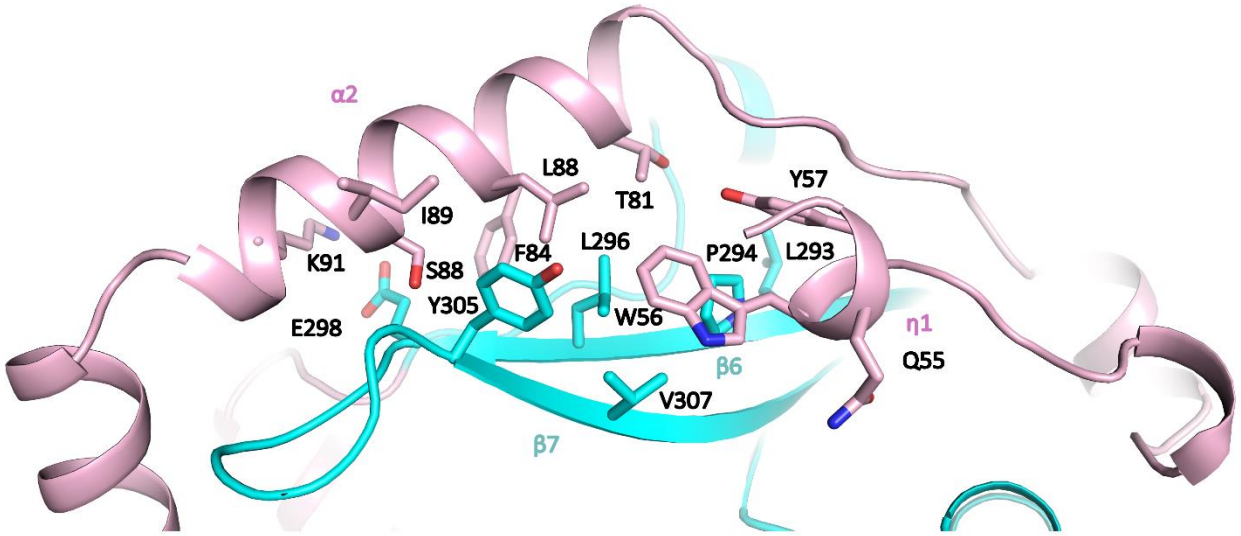

Supplementary Figure S1. Stabilization of the DREV core domain by the N-terminal motif of METTL9. The N-terminal motif of METTL9 is colored pink and the DREV core domain is colored cyan. Key residues are depicted as sticks.

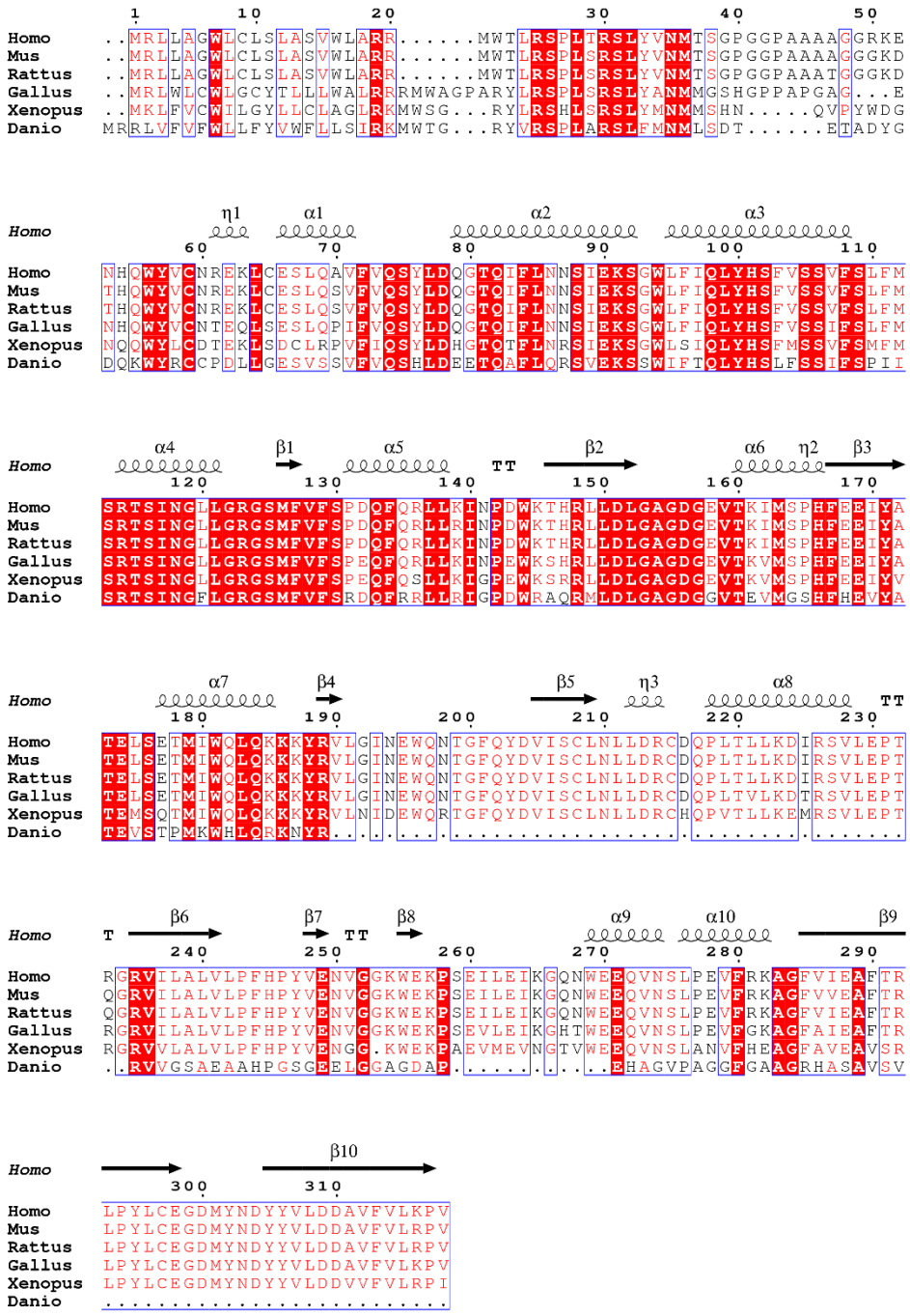

Supplementary Figure S2. Sequence alignment of METTL9 among different species. Consistent sequences are shown in white on a red background, similar sequences are shown in red on a white background, α helix is shown as a helix, β sheet is shown as an arrow, and the names are marked above.

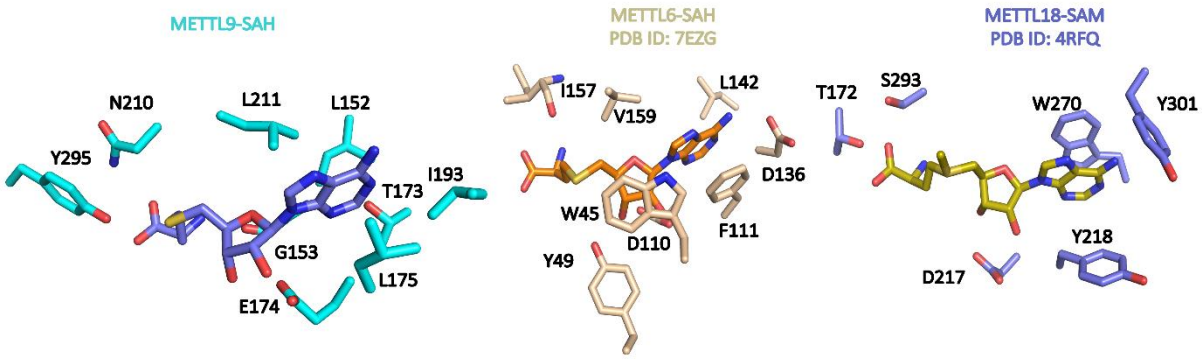

Supplementary Figure S3. SAH binding of METTL9 with other methyltransferases. SAH binding patterns of METTL9 (left), METTL6 (middle), and METTL18 (right).

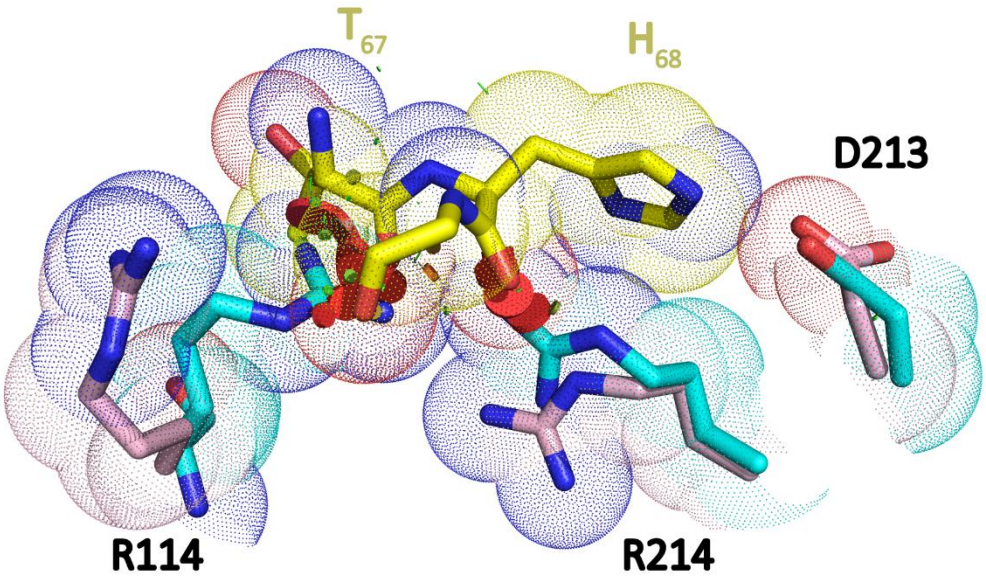

Supplementary Figure S4. Shift of R114 and R214 due to the substrate binding. Residues of free METTL9 are colored in cyan and residues of substrate-bound METTL9 are colored in pink, substrate residues are colored in yellow. Residues are highlighted in the “dotted” van der Waals radius representation. Clashes are presented in red Cylinders.

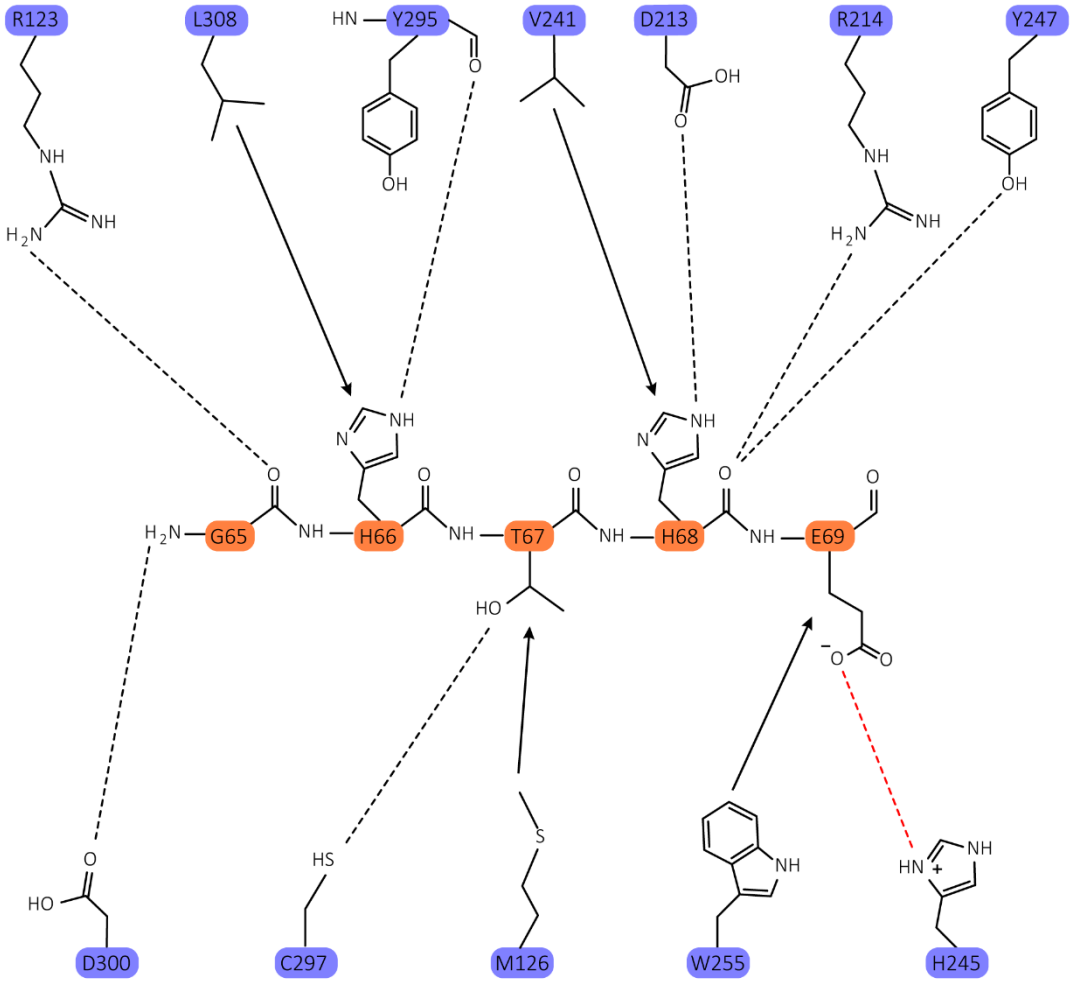

Supplementary Figure S5. Schematic representation of METTL9 interactions with the SLC39A7$_{65\text{-}69}$ peptide. Residues of SLC39A7 peptide are shown in orange, and METTL9 residues are shown in blue. Hydrophobic interactions are indicated by arrows, hydrogen bonds are indicated by black dashed lines, and salt bridge is indicated by red dashed lines.

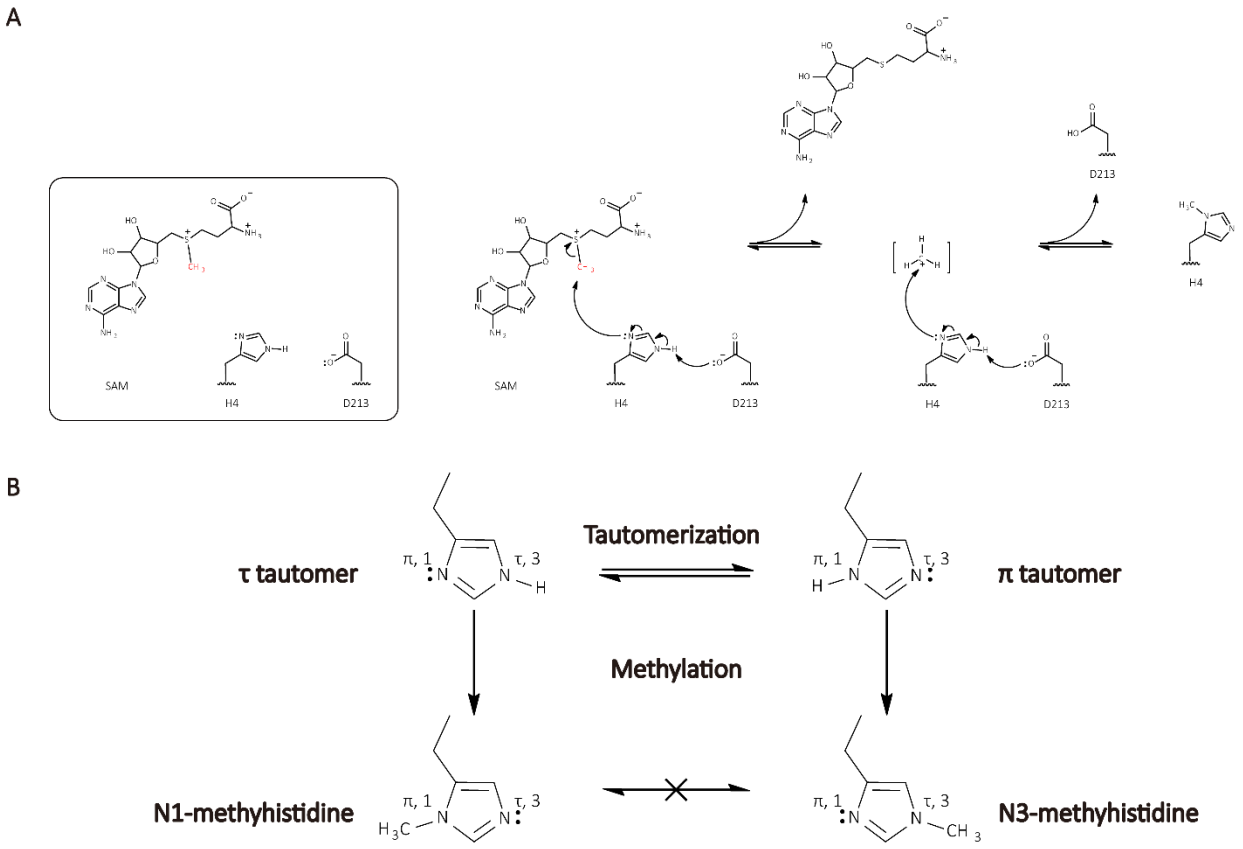

Supplementary Figure S6. Chemical property of methylation on histidine. **(A)** Formation of hydrogen bonding interaction of H_i with D213 influences site-specific methylation of histidine. **(B)** Methylation on either Nπ or Nτ will block the tautomerization of histidine.

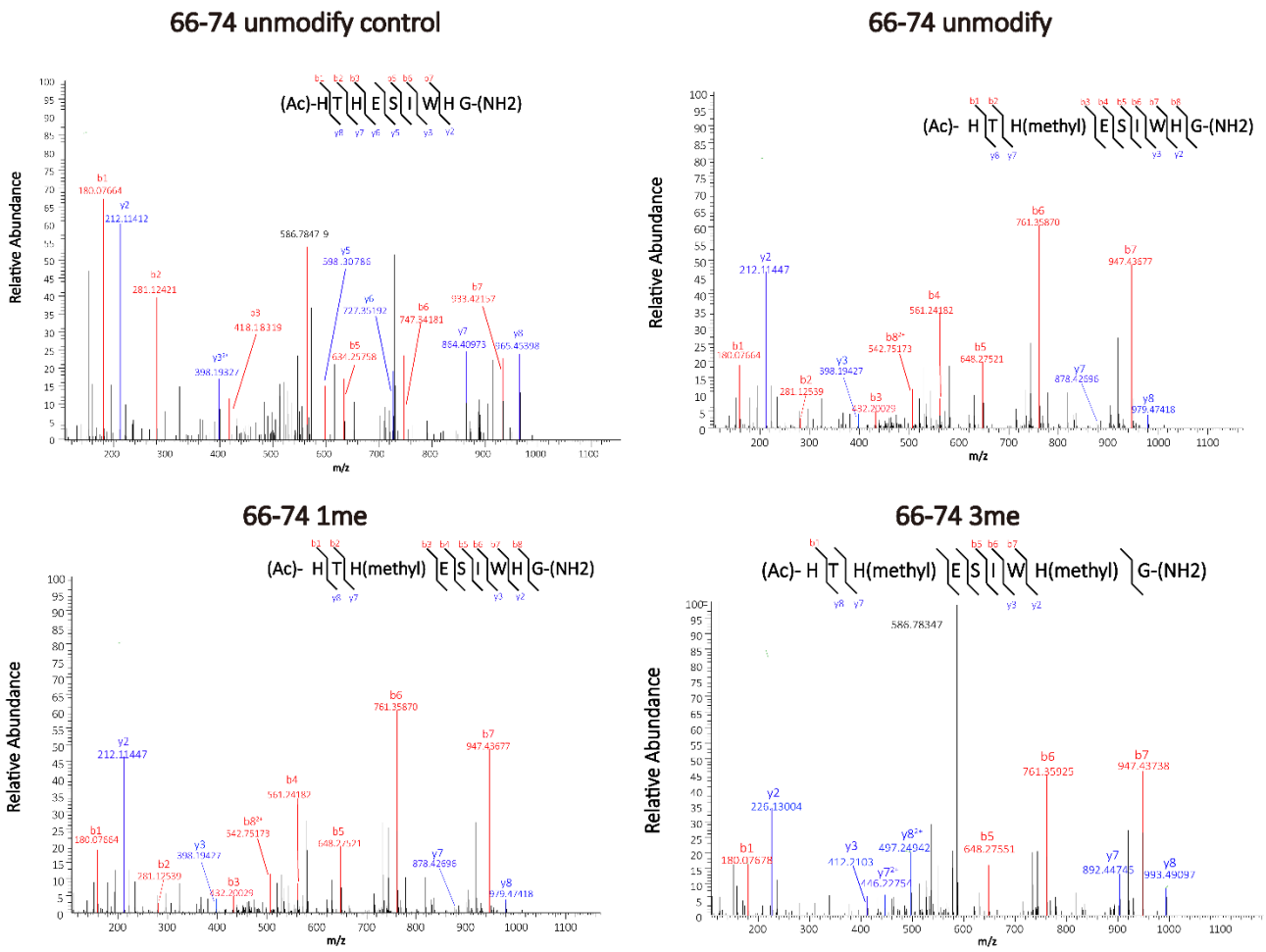

Supplementary Figure S7. LC-MS/MS results of METTL9 catalyzed methylation of SLC39A7$_{66\text{-}74}$ peptides. Substrates of each reaction are labeled on top. Peaks corresponding to fragments are highlighted. b-ion fragments are colored in red, and y-ion fragments are colored in blue.

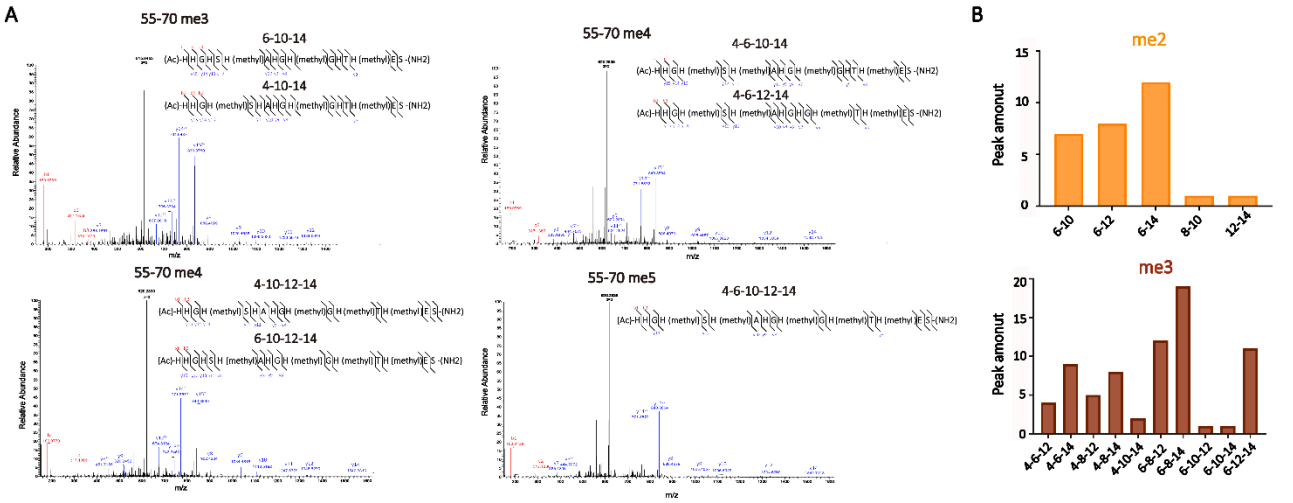

Supplementary Figure S8. Analysis of METTL9 catalyzed time-course methylation of SLC39A7$_{55\text{-}70}$ peptides **(A)** LC-MS/MS results of METTL9 catalyzed time-course methylation of SLC39A7$_{55\text{-}70}$ peptides. Substrates of each reaction are labeled on top. Peaks corresponding to fragments are highlighted. b-ion fragments are colored in red, and y-ion fragments are colored in blue. **(B)** LC-MS/MS analysis of methylation pattern for di- and tri-methylation products. X-axis presents different methylation pattern; Y-axis presents peak amount searched from LC-MS/MS results.

Supplementary Table S1. Data collection and refinement statistics

	METTL9$_{37-318}$-SAH	METTL9$_{37-318}$-SAH-SLC39A7$_{65-70}$
PDB code	8GZE	8GZF
Data collection		
Wavelength (Å)	0.9792	0.9792
Space group	$P6_1$	$P6_122$
Cell dimensions		
a, *b*, *c* (Å)	109.8, 109.8, 120.3	79.2, 79.2, 422.4
α, *β*, *γ* (°)	90, 90, 120	90, 90, 120
Resolution (Å)	50-2.5 (2.54-2.50)*	50-3.4 (3.46-3.40)
R_{merge} (%)	10.7 (94.2)	19.7 (73.9)
$I / \sigma I$	39.1 (2.59)	6.1 (1.48)
Completeness (%)	100.0 (100.0)	96.1 (93.7)
Redundancy	17.0 (17.9)	5.2 (5.6)
Refinement (F>0)		
Resolution (Å)	28.7-2.50	17.3-3.40
No. of reflections	28,299	11,178
R_{work} / R_{free} (%)	19.0/24.1	25.5/30.5
No. of atoms		
Protein	4368	4342
SAH/peptide	52/-	52/80
Water	105	0
B-factors (Å^2)		
Protein	69.7	69.6
SAH/peptide	44.7/-	61.6/67.4
Water	52.9	-
R.m.s. deviations		
Bond lengths (Å)	0.002	0.003
Bond angles (°)	0.566	0.775
Ramachandran Plot		
Favored (%)	96.59	96.05
Allowed (%)	3.41	3.95
Outliers (%)	0	0

*Statistics for the highest-resolution shell are shown in parentheses

Supplementary Table S3. Peptides used in this article.

Peptide segment	Peptide sequence	Usage
HGHS	Ac-HGHS-NH_2	ITC assay
$SLC39A7_{65\text{-}70\ un}$	Ac-GHTHES-NH_2	Crystal growth
$SLC39A7_{66\text{-}74\ un}$	Ac-HTHESWIHG-NH_2	Enzymatic assay
$SLC39A7_{66\text{-}74\ N1\text{-}me}$	Ac-HTH (N1-methyl) ESWIHG-NH_2	Enzymatic assay
$SLC39A7_{66\text{-}74\ N3\text{-}me}$	Ac-HTH (N3-methyl) ESWIHG-NH_2	Enzymatic assay
$SLC39A7_{66\text{-}74\ Hi\text{-}2\text{-}N1me}$	Ac-H (N1-methyl) THESWIHG-NH_2	Enzymatic assay
$SLC39A7_{66\text{-}74\ Hi\text{-}2\text{-}N\tau me}$	Ac-H (N3-methyl) THESWIHG-NH_2	Enzymatic assay
$SLC39A7_{66\text{-}74\ Hi\text{-}2\ to\ X}$	Ac-XTHESWIHG-NH_2 (X represents the other 19 amino acids)	Enzymatic assay
$SLC39A7_{243\text{-}255\ un}$	Ac-GHGHSHGHGHAHS-NH_2	Enzymatic assay

Supplementary Table S4. Thermodynamic parameters of representative ITC titrations.

METTL9	Ligand	ΔH(cal·mol^{-1})	-TΔS(cal·mol^{-1})	ΔG(cal·mol^{-1})
WT	SAM	-6030	-1651.0465	-7681.0465
WT	SAH	-1.91E+04	11826.235	-7293.765
T173A	SAH	-1.27E+04	5935.89	-6804.11
T115A	SAH	-1.06E+04	4034.1	-6575.9
N118A	SAH	-2.23E+04	16395.735	-5914.265
D156A	SAH	N.D.		
N210D	SAH	N.D.		
R214D	SAH	N.D.		
Y295A	SAH	N.D.		
D151A	SAH	N.D.		
WT	HGHS	-1.64E+04	9153.205	-7276.795
Y247A	HGHS	-1562	-5664.85	-7226.85
C297A	HGHS	-4.00E+04	33690.95	-6269.05
N118A	HGHS	N.D.		
R123A	HGHS	N.D.		
R214D	HGHS	N.D.		
T115A	HGHS	-3261	-2981.5	-6242.5
V241G	HGHS	-7006	1171.7295	-5834.2705
M126A	HGHS	N.D.		
E249A	HGHS	N.D.		
D213A	HGHS	N.D.		
D213N	HGHS	-6.55E+03	341.197	-6208.803
D213S	HGHS	-1.11E+04	5146.87	-5973.13